

AD-A129 748

MECHANICAL PROPERTIES AND FRACTOGRAPHY OF ELECTROSLAG
REMELED 300M STEEL(U) ARMY MATERIALS AND MECHANICS
RESEARCH CENTER WATERTOWN MA A A ANCTIL MAR 83

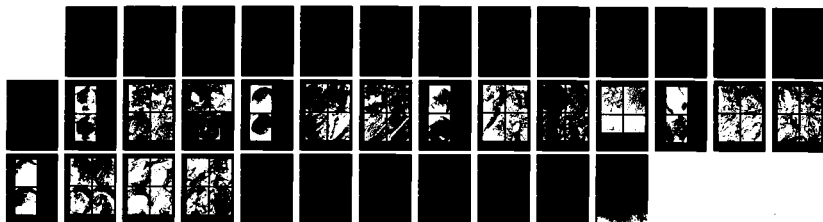
1/1

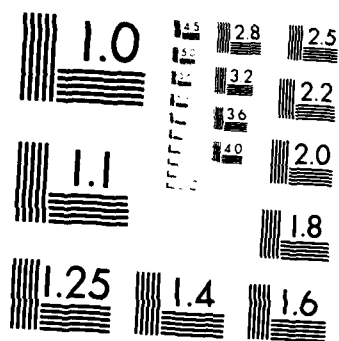
UNCLASSIFIED

AMMRC-TR-83-13

F/G 11/6

NL





MICROCOPY RESOLUTION TEST CHART
NATIONAL BUREAU OF STANDARDS 1010-A

ADA 1237

AMMRC TR 83-13

AD

MECHANICAL PROPERTIES AND FRACTOGRAPHY OF ELECTROSLAG REMELTED 300M STEEL

ALBERT A. ANCTIL
METALS RESEARCH DIVISION

March 1983

Approved for public release; distribution unlimited.

ARMY MATERIALS AND MECHANICS RESEARCH CENTER
Watertown, Massachusetts 02172

DTIC FILE COPY

The findings in this report are not to be construed as an official Department of the Army position, unless so designated by other authorized documents.

Mention of any trade names or manufacturers in this report shall not be construed as advertising nor as an official indorsement or approval of such products or companies by the United States Government.

DISPOSITION INSTRUCTIONS

Destroy this report when it is no longer needed.
Do not return it to the originator.

SECURITY CLASSIFICATION OF THIS PAGE (When Data Entered)

DD FORM 1473 EDITION OF 1 NOV 55 IS OBSOLETE
1 JAN 73

SECURITY CLASSIFICATION OF THIS PAGE (When Data Entered)

UNCLASSIFIED

SECURITY CLASSIFICATION OF THIS PAGE(When Data Entered)

Block No. 20

ABSTRACT

Engineering and stress corrosion cracking properties, with microscopic examination of fracture surfaces, are presented for a high strength electroslag remelted 300M steel. Comparisons are made of electroslag remelted 4340 steel and electroslag and vacuum arc remelted 300M and 4340 steels. Electroslag remelted 300M steel at high strength levels can achieve the mechanical property levels obtained by vacuum arc remelting in the longitudinal orientation. However, the short transverse ductility of electroslag remelted 300M steel varies considerably and can be unacceptably low. Scanning electron microscopic examination of short transverse tensile specimens having good ductility did not reveal any fractographic differences that could be related to the heat treatment process. Impact energy varied with orientation. No improvement in stress corrosion cracking susceptibility was obtained over VAR 4340 steel.

UNCLASSIFIED

SECURITY CLASSIFICATION OF THIS PAGE(When Data Entered)

CONTENTS

	Page
INTRODUCTION.	1
MATERIAL.	1
RESULTS AND DISCUSSION	
Mechanical Properties.	2
Stress Corrosion Cracking.	3
Fractography	5
CONCLUSIONS	6
ACKNOWLEDGMENT.	7

INTRODUCTION

Electroslag remelted (ESR) 4340 steel has been chosen for ballistically resistant and tolerant components of the advanced attack helicopter (AAH).¹ Heat to heat variations, in some cases, have resulted in unacceptably low short transverse mechanical properties, i.e., elongation less than 10 percent and reduction-of-area less than 25 percent, at ultimate strength levels exceeding 260 ksi.

Other processing techniques and alloys are being considered as substitutes for the ESR 4340 steel. The British Steel Corporation (BSC) has proposed an ESR 300M steel.² This alloy is a modified 4340 steel used in many aerospace applications, containing 1.6 weight percent silicon with the addition of vanadium and minor increases in carbon and molybdenum. The 300M steel alloy is used primarily in the form of bar, tubing, and forging stock at the ultimate strength range of 270 ksi to 300 ksi.

A 4" x 6" x 6" forging of 300M steel was provided by the BSC for mechanical property and ballistic characterization. This report summarizes the mechanical property study.

MATERIAL

The chemical composition of this heat was provided by the BSC and is shown in Table 1. The carbon content is considered low for this alloy. Test specimens were first machined in blank form and then heat treated. The heat treatment consisted of normalizing at 1700°F - 1 hour air cooled; tempering at 1200°F - 1 hour air cooled; austenitizing at 1600°F - 1 hour oil quenched; and double tempering at 570°F for 2+2 hours air cooled.

An additional set of short transverse specimens was normalized 1-3/4 hours and austenitized 2 hours in a vacuum at the same temperatures by Hughes Helicopters. These specimens were then double tempered in a vacuum for 4+4 hours at 575°F.

All of the specimen blanks were then finished machined and tested in accordance with the American Society for Testing and Materials (ASTM) standard methods.

Table 1. CHEMICAL COMPOSITION, WEIGHT PERCENT

C	Mn	Si	Ni	Cr	Mo	V	P	S	Al	Cu	As	Sn	Co
0.40	0.87	1.61	1.83	0.77	0.36	0.08	0.008	0.006	0.017	0.13	0.024	0.009	<0.02

1. *The Application of Electroslag Refined 4340 Steel to Structural and Ballistic Requirements for the Advanced Attack Helicopter.* Hughes Helicopters, Report HH79-91, April 1979.
2. HARRIS, D., and PRIEST, A. H. *The Evaluation of ESR 300M Steel for Use in Aircraft Carriages.* British Steel Corporation, Sheffield Division, Stockbridge and Tinsley Park Works, Stockbridge, Sheffield S30 5JA, Report No. PROD/EM/1/79, January 1979.

RESULTS AND DISCUSSION

Mechanical Properties

The minimum mechanical properties specified by Hughes Helicopters [Hughes Materials Specification (HMS 6-1121)] for ballistically critical components of the AAH are tabulated in Table 2.*

Mechanical properties obtained from the ESR 300M steel are given in Table 3. Data from Table 3 have been averaged and are compared with similar mechanical property data from other sources in Table 4.

The longitudinal ESR 300M strength and ductility properties meet or exceed the minimum specified values. Yield and ultimate strength levels exceed the minimum requirements in both the short and long transverse orientations. In the long transverse direction the percent reduction-of-area exceeds the 25 percent (one exception) requirement while the percent elongation falls short of the required 10 percent. Ductility in the short transverse direction for material heat treated in air is poor and erratic, failing to meet the criteria with any consistency. However, material treated in a vacuum did result in consistent ductility values. In each case, the reduction-of-area exceeds the 25 percent present requirement; nevertheless, the average elongation, 8.1 percent, does not reach the 10 percent level called for. The percent reduction-of-area obtained from the vacuum heat treatment and those obtained by the BSC compare favorably with VAR 300M and ESR and VAR 4340 steels listed in Table 4.

Longitudinal tensile properties compare favorably with those reported by Harris and Priest² for ESR 300M and by Wells et al.⁴ for VAR 300M. A favorable comparison also exists for ESR 300M versus ESR and VAR 4340 steel heats listed in Table 4.^{†4-6}

Short transverse data from a particular heat of ESR 4340 steel evaluated at AMMRC have been included to illustrate the variation in ductility that is possible.⁶ Average longitudinal properties determined for this heat are 212 ksi, 0.2% Y.S.; 317 ksi, U.T.S; 10% elongation, and 38% reduction-of-area.

Table 2. MINIMUM MECHANICAL PROPERTIES

	0.2% Y.S. (ksi)	U.T.S. (ksi)	Elong. (%)	R.A. (%)	HRC	K _{IC} (ksi√in.)
Short Transverse	200	260	10	25	54-57	50
Longitudinal	200	280	10	25	54-57	50

*Hughes Helicopters Process Specification, HMS 6-1121.

†NEHRENBURG, A. E. *Properties of ESR 4340*, presented at the ASM Seminar on Electroslag Remelting, Los Angeles, California, December 1979.

3. WELLS, M. G. H., HAUSER, J. J., and PERLMUTTER, I. *Effect of Cleanliness and Process Variables on the Fracture Toughness of 4340 and 300M Billets*. ASM Fracture Prevention and Control, Book 3, 1974.
4. ANCTIL, A. A., and RUDY, F. J. *Engineering and True Stress-Strain Tensile Properties of High Strength ESR 4340 and 4350 Steels*. AMMRC SP 75-9, November 1975.
5. RITCHIE, R. O., CASTRO CEDENO, M. H., ZACKAY, V. F., and PARKER, E. R. *Effects of Silicon Additions and Retained Austenite on Stress Corrosion Cracking in Ultrahigh Strength Steels*. Metallurgical Transactions, v. 9A, p. 35, no. 1, January 1978.
6. OLSON, G. B., ANCTIL, A. A., DeSISTO, T. S., and KULA, E. B. *Anisotropic Embrittlement in High-Hardness ESR 4340 Steel Forgings*. AMMRC TR 82-1, January 1982.

Table 3. MECHANICAL PROPERTIES

Orientation	0.1% Y.S. (ksi)	0.2% Y.S. (ksi)	T.S. (ksi)	Elong. %	R.A. %	Impact Energy ft-lb	HRC
Longitudinal	224	239	287	10.7	45.7	21	55
	219	236	284	10.7	43.7	19	54
	224	240	291	10.7	40.9	18	54
	234	251	294	10.7	44.1	20	55
	221	236	284	10.7	46.3		
	242	258	299	10.7	43.7		
	229	246	297	9.4	41.3		
	237	250	292	11.4	45.6		
Long Transverse	243	258	295	9.0	51.4	17	55
	231	251	295	9.0	50.7	19	54
	227	245	292	9.0	50.4	18	54
	233	251	295	9.0	50.7	14	54
	230	249	293	9.0	50.4		
	224	252	296	9.0	50.7		
	242	258	296	9.0	50.7		
	237	252	296	9.0	50.7		
Short Transverse	231	247	295	9.0	50.7	17	55
	233	252	295	9.0	50.7	18	55
	225	241	289	9.0	50.4	16	55
	239	255	296	9.0	50.4	17	55
	230	247	295	9.0	50.7		
	226	241	292	4.6	53.4		
	225	244	290	5.1	50.1		
	225	244	287	5.3	57.4		
Short Transverse*	228	243	286	8.2	30.3		
	225	239	285	9.1	32.2		
	233	250	288	9.0	33.4		
	227	243	288	7.3	29.4		
	224	238	281	7.9	34.8		
	224	237	280	7.4	32.2		
	231	244	283	7.6	31.4		
	231	244	288	9.1	33.4		

*Vacuum heat treated by Hughes Helicopters.

All ESR 300M long and short transverse elongation values failed to meet the 10 percent requirement and six of the eight short transverse tensile specimens heat treated in air failed to meet the 25 percent reduction-of-area minimum requirement. Reduction-of-area values for short transverse vacuum heat-treated samples exceeded the minimum requirements.

Charpy impact energy values shown in Table 3 varied from a high of 22 ft-lb for the L-T orientation to 9 ft-lb for the S-L orientation.

Stress Corrosion Cracking

Stress corrosion cracking (K_{ISCC}) tests were performed under constant load in a 3.5 percent solution of sodium chloride at room temperature. A 3.0-inch-long by 0.4-inch-wide by 0.2-inch-thick specimen with a precracked edge notch was used. Heat treatment was in air. The stress corrosion test results are tabulated in Table 5. Plots of stress intensity versus time to failure for longitudinal and transverse specimen orientations are shown in Figures 1a and 1b.

Table 4. MECHANICAL PROPERTIES OF 300M AND 4340 STEELS

Alloy	Temp. (°F)	Orien- tation	0.2% Y.S. (ksi)	U.T.S. (ksi)	Elong. (%)	R.A. (%)	Impact Energy (ft-lb)	K _{IC} (ksi√in.)	K _{ISCC} (ksi√in.)	Reference
ESR 300M*	570	longitudinal	245	290	10-11	41-46	20	—	11	Anctil
ESR 300M	570	longitudinal	238	281	11	45	—	50	14	Harris - Priest ²
VAR 300M	600	longitudinal	259	302	—	48	—	52	—	Wells et al. ³
ESR 300M*	570	long trans.	252	295	6-9	23-33	15	—	—	Anctil
ESR 300M*	570	short trans.	246	292	4-8	11-29	14	—	11	Anctil
ESR 300M*	575†	short trans.	242	285	7-9	29-35	—	—	—	Anctil
ESR 300M	570	short trans.	241	283	8	38	—	48	13	Harris - Priest ²
VAR 300M	600	trans. round	250	300	8-10	25-30	—	45	10	McDarmaid ⁷
VAR 300M	600	trans. round	255	292	—	34	—	57	—	Wells et al. ³
ESR 4340	450	longitudinal	235	295	13	43	19	61	—	Anctil - Rudy ⁴
VAR 4340	400	longitudinal	215	290	14	46	15	59	—	Nehrenberg†
VAR 4340	400	longitudinal	241	294	—	50	—	53	—	Wells et al. ³
VAR 4340	390	longitudinal	233	302	14	—	—	60	15	Ritchie et al. ⁵
ESR 4340	375	long trans.	216	283	13	45	—	60	—	Anctil - Rudy ⁴
ESR 4340	400	long trans.	215	295	11	35	11	57	—	Nehrenberg†
ESR 4340	340	short trans.	220	315	0-10	0-16	9	40	—	Olson et al. ⁶
VAR 4340	400	trans. round	240	294	—	38	—	55	—	Wells et al. ³

*Average values from Table 3

†Heat treated in vacuum

NEHRENBURG, A.E. Properties of ESR 4340, presented at the ASM Seminar on Electroslag Remelting, Los Angeles, California, December 1979.

Table 5. ESR 300M STRESS CORROSION DATA

						$K = \frac{P\sqrt{a}}{BW} \cdot Y$ K = stress intensity factor P = load Y = finite width correction		
Orien- tation	B (in.)	W (in.)	a (in.)	$\frac{a}{W}$	$f\left(\frac{a}{W}\right)$	P (lb)	K (ksi√in.)	T _f (hr)
L-T	0.200	0.400	0.166	0.415	3.91	938	18.7	0.5
	0.200	0.400	0.173	0.433	4.10	654	13.9	71.1
	0.200	0.399	0.170	0.426	4.02	735	15.3	226.4
	0.200	0.400	0.165	0.406	3.86	628	12.3	754.5
	0.200	0.400	0.161	0.403	3.78	500	9.5	1,006.8*
S-T	0.200	0.400	0.163	0.408	3.83	968	18.7	0.9
	0.200	0.400	0.168	0.420	3.95	745	15.1	251.5
	0.200	0.400	0.155	0.388	3.63	719	12.8	388.5
	0.200	0.400	0.157	0.393	3.68	653	11.9	788.1
	0.200	0.400	0.162	0.405	3.80	500	9.5	1,006.9*

*no failure

$$K_{ISCC} \text{ (L-T)} = 11 \text{ ksi}\sqrt{\text{in.}}$$

$$K_{ISCC} \text{ (S-T)} = 11 \text{ ksi}\sqrt{\text{in.}}$$

7. McDARMAID, D. S. *Effects of Different Austenitization Treatments on K_{IC}, K_{ISCC} and Other Mechanical Properties of 300M Steel Bar.* Metals Technology, p. 7, January 1978.

The value of K_{ISCC} was independent of specimen orientation. This was also the case for data reported by Harris and Priest.² The K_{ISCC} value of $11 \text{ ksi}\sqrt{\text{in.}}$ was $2 \text{ ksi}\sqrt{\text{in.}}$ units lower in each case than that obtained by Harris and Priest. The stress corrosion fracture mode was intergranular. No significant difference in K_{ISCC} is noted for ESR or VAR 300M or the 4340 steels shown in Table 4. The addition of silicon did not improve the stress corrosion cracking resistance for the heat of ESR 300M over that of the $15 \text{ ksi}\sqrt{\text{in.}}$ value reported by Ritchie et al.⁵ for VAR 4340 steel at approximately the same strength level. Ritchie obtained a value of $17 \text{ ksi}\sqrt{\text{in.}}$ for VAR 300M at this strength level.

Fractography

Typical tensile fracture surfaces from the longitudinal, long transverse, and short transverse orientations were examined under the scanning electron microscope (SEM). Figures 2, 3, 4, 5, and 6 show a macroscopic photograph of the tensile fracture surface and the SEM areas examined. The stringers mentioned in the following discussion were identified as manganese sulfides (MnS) by the SEM EDAX spectrometer. The traces are shown in Figure 4k.

The longitudinal tensile fracture surface shown in Figure 2 has a full shear lip. The fracture mode is predominantly dimpled rupture. Typically, the fracture surface has a rough appearance (Figure 2a). Secondary cracking is observed along the tensile axis (Figures 2b and 2f). MnS cleavage planes can be seen in Figures 2b and 2d. Large voids, nucleated by MnS inclusions, were seen. One such void, surrounded by dimpled rupture, is shown in Figure 2e. A SEM photograph of the shear lip (Figure 2g) shows a fine network of elongated dimples with the presence of larger voids.

The long transverse tensile specimen failed in a ductile cup and cone fashion. The surface reveals a textured pattern corresponding to the major working direction of the forging. Shear planes extending into the long transverse direction can be seen in Figure 3e. These shear plane fractures may have been initiated by MnS inclusions (Figure 3b). Manganese sulfide troughs, some still containing sulfide particles, can be seen at various locations on the fracture surface (Figures 3a, 3b, 3c and 3d). Elongated dimples (Figure 3g) and a uniform change in the fracture plane (Figure 3h) were observed on the shear lip.

The tensile fracture in the short transverse orientation for material heat treated in air and having poor ductility developed a nearly continuous ductile shear lip (Figure 4). It also has a textured appearance. The fracture origin was located at the intersection of a MnS inclusion with the specimen surface (Figure 4a). The structure shown in Figures 4b and 4d, taken close to the fracture origin, is quasi-cleavage. The inclusion shown in Figure 4c was identified with the SEM spectrometer as MnS (Figure 4k). An array of MnS inclusions or troughs can be seen in Figure 4e measuring from 0.003 inch to 0.005 inch. Dimpled rupture, void formation, and some cleavage is observed in Figures 4g and 4h. Lastly, typical elongated fine dimples are seen on the shear lip (Figure 4j).

Six of the eight tensile fracture surfaces examined showed that the fracture initiated at the specimen surface. Further, in four of the six specimens, the initiation was caused by the intersection of an inclusion with the surface.

Fractographs of the fracture surface of a specimen machined in the short transverse orientation from material heat treated in an air furnace are shown in Figure 5. The specimen had a 29 percent reduction-of-area at fracture. The tensile fracture originated at the center with radial propagation to the final separation by ductile shearing. The central area is shown in Figure 5a with an enlargement in Figure 5b showing an inclusion surrounded by dimples. Figures 5c and 5d show an area containing large voids which have coalesced. Pores and voids are visible in Figures 5e, 5f, and 5g. Some evidence of quasi-cleavage and dimples can be seen in Figure 5h.

SEM micrographs of a specimen having 33 percent reduction-of-area and heat treated in vacuum are shown in Figure 6. The fracture, which initiated internally, has radial markings and is separated by ductile shearing. The fracture appearance was rougher than its companion specimens heat treated in air. Large pores and voids can be seen in the initiation zone (Figures 6a and 6b). An inclusion initiated pore can be seen in Figures 6c and 6d. Fracture progressed by microvoid coalescence as evidenced in Figure 6e, 6f, and 6g. Figure 6 shows an inclusion surrounded by an immediate zone of quasi-cleavage giving way to dimpled rupture.

Heat treatment in air or vacuum had no effect on the fracture surface morphology of short transverse tensile specimens that exceeded minimum ductility requirements. Significantly, more elongated inclusions with evidence of quasi-cleavage were observed in the fractures initiating at the surface in specimens heat treated in air and having poor ductility.

SEM photographs of fracture surfaces of longitudinal (L-T) K_{ISCC} specimens are shown in Figure 7. The fracture mode evident in Figures 7a through 7c is intergranular. Figure 7d, taken from the fast fracture zone of the test specimen, shows a ductile or dimpled fracture mode.

CONCLUSIONS

1. Electroslag remelted 300M steel at high strength levels can achieve the mechanical property levels obtained by vacuum arc remelting in the longitudinal orientation. However, the short transverse ductility of electroslag remelted 300M steel varies considerably and can be unacceptably low.
2. The longitudinal strength and ductility met and exceeded the required minimum values. The results were comparable to other heats of ESR or VAR 300M and 4340 steels.
3. The yield and ultimate strength levels in both the short and long transverse orientations exceed the required values and compare favorably to other heats of ESR or VAR 300M and 4340 steels.
4. Long transverse ductility (% R.A.) was marginally acceptable. However, the percent elongation did not attain the required amount.
5. Short transverse ductility (% R.A., % Elon.) for material heat treated in air was poor and erratic, failing to meet the criteria.
6. Erratic and poor short transverse ductility is caused by the random intersection of the specimen surface with MnS inclusions.

7. Short transverse ductility for material heat treated in vacuum met the reduction-of-area requirement consistently but with lower than required elongation values. No explanation is offered for this behavior.

8. Impact energy varied with orientation.

9. No improvement in stress corrosion cracking susceptibility was obtained over VAR 4340 steel.

10. Scanning electron microscopic examination of short transverse tensile specimens having good ductility did not reveal any fractographic differences that could be related to the heat treatment process.

ACKNOWLEDGMENT

This report is the product of a jointly planned and coordinated effort under cognizance of the Joint Technical Coordinating Group on Aircraft Survivability (JTCG/AS), Naval Air Systems Command, Code 5204J, Washington, D.C. 20361. The JTCG/AS is a chartered activity under the aegis of the Joint AMC/NMC/AFLC/AFSC Logistics Commanders. JTCG/AS Project ID No. TA-1-02.0 Experimental Armor Materials.

The author acknowledges the helpful discussions with Mr. Thomas S. DeSisto and the assistance of Mr. Walter F. Czyrkliis who obtained the stress corrosion cracking data.

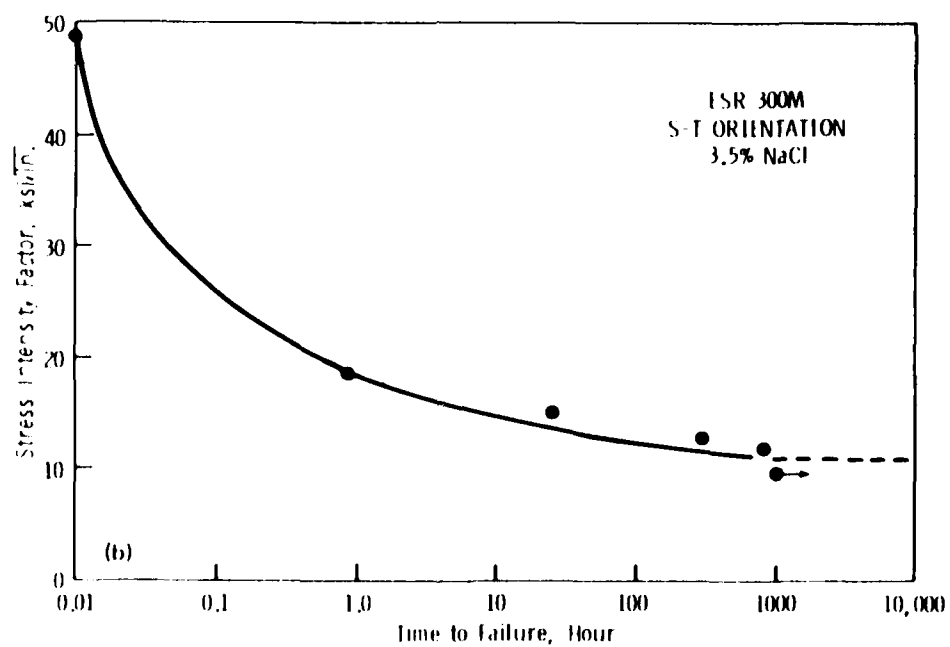
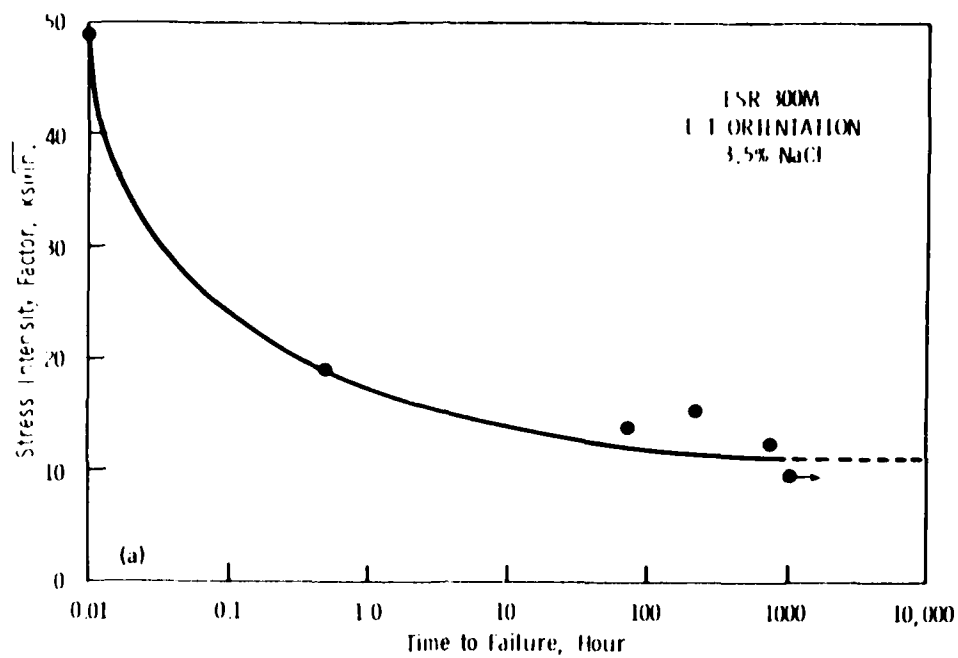


Figure 1. Stress intensity versus time for stress corrosion cracking.



20X

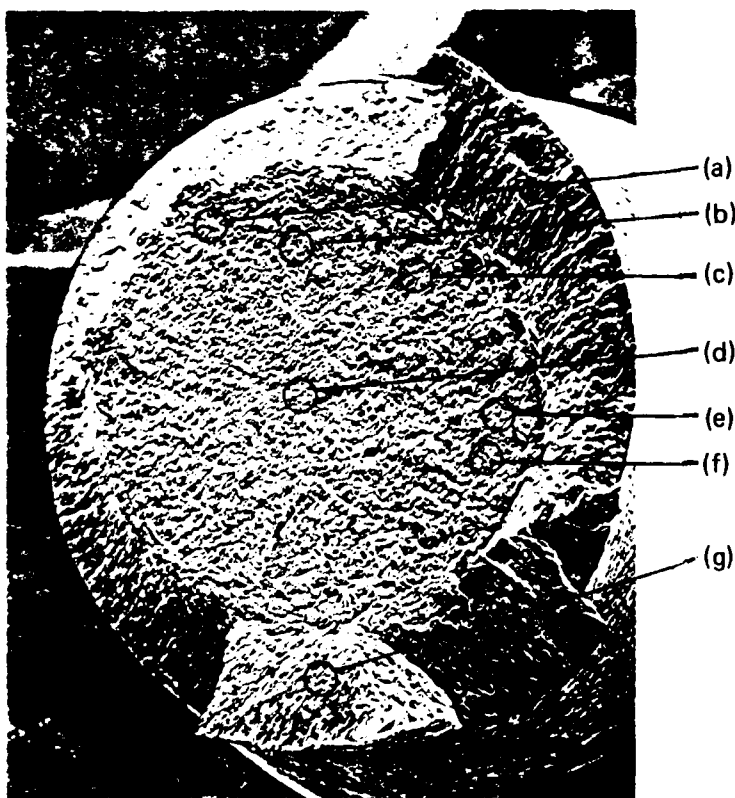
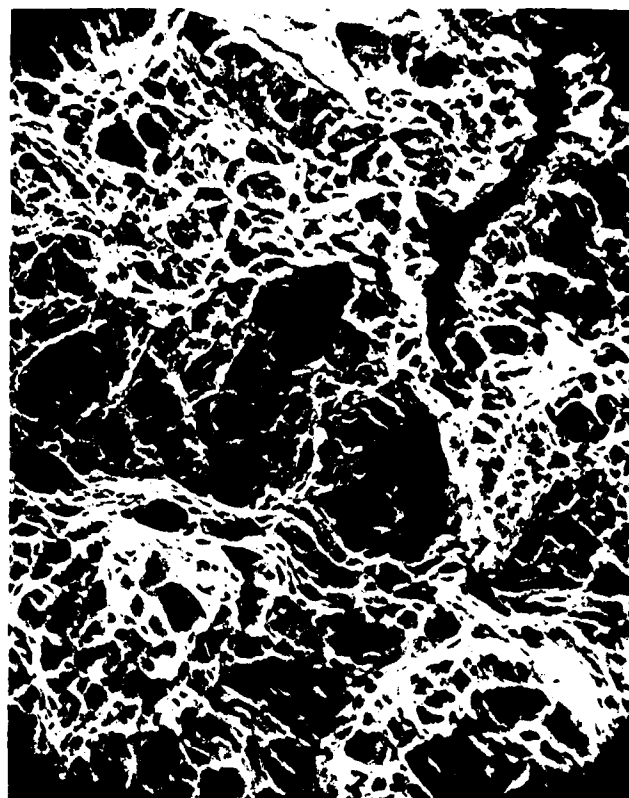


Figure 2. SEM longitudinal
tensile fractographs.
ESR 300M, longitudinal.



(a)

200X



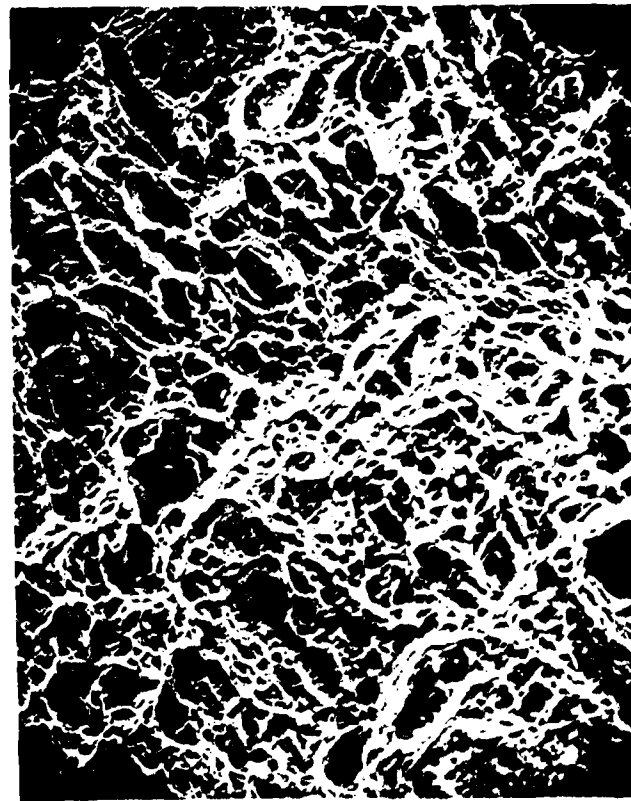
(b)

2000X



(c)

1000X



(d)

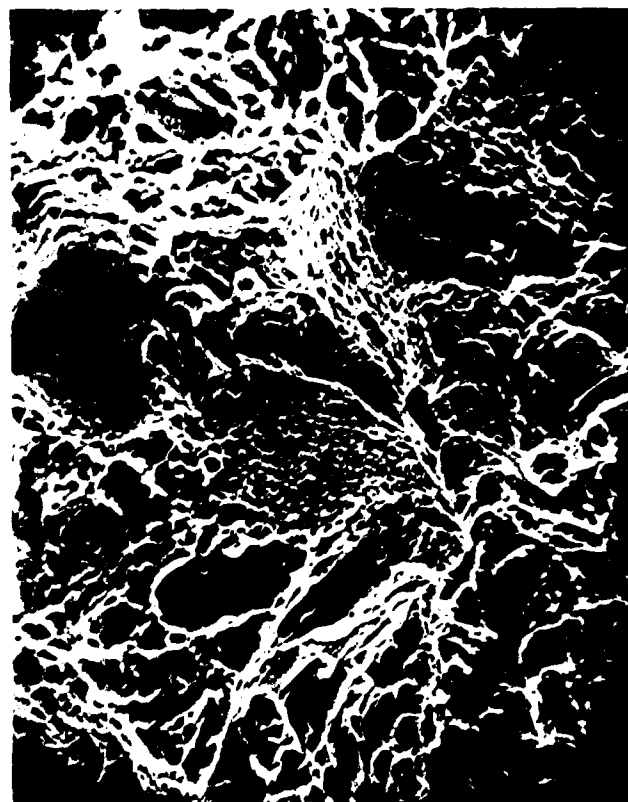
2000X

Figure 2. ESR 300M, longitudinal (cont.).



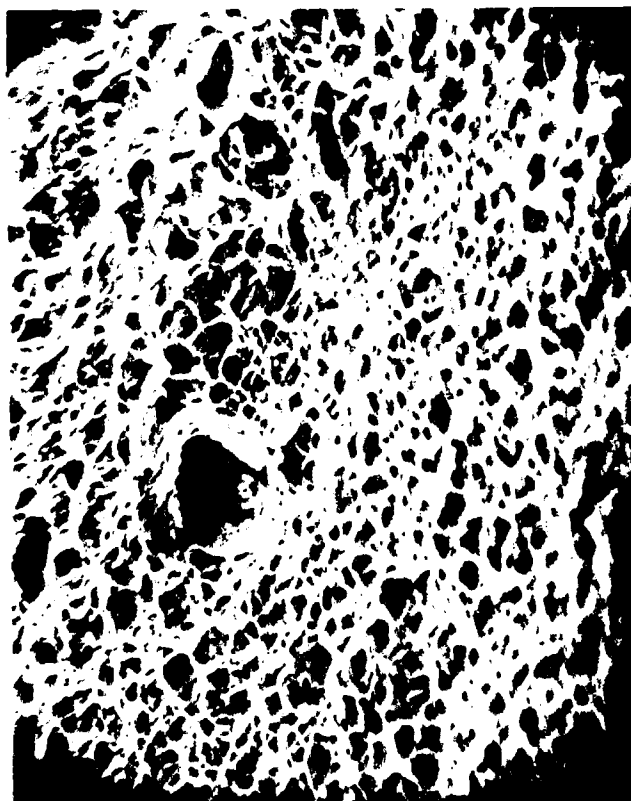
(e)

2000X



(f)

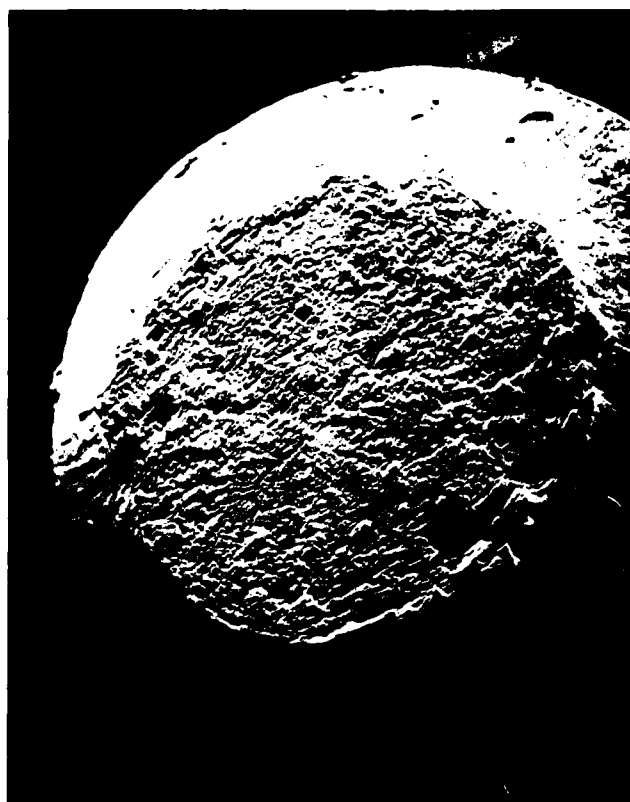
2000X



(g)

5000X

Figure 2. ESR 300M (longitudinal (cont.)).



20X

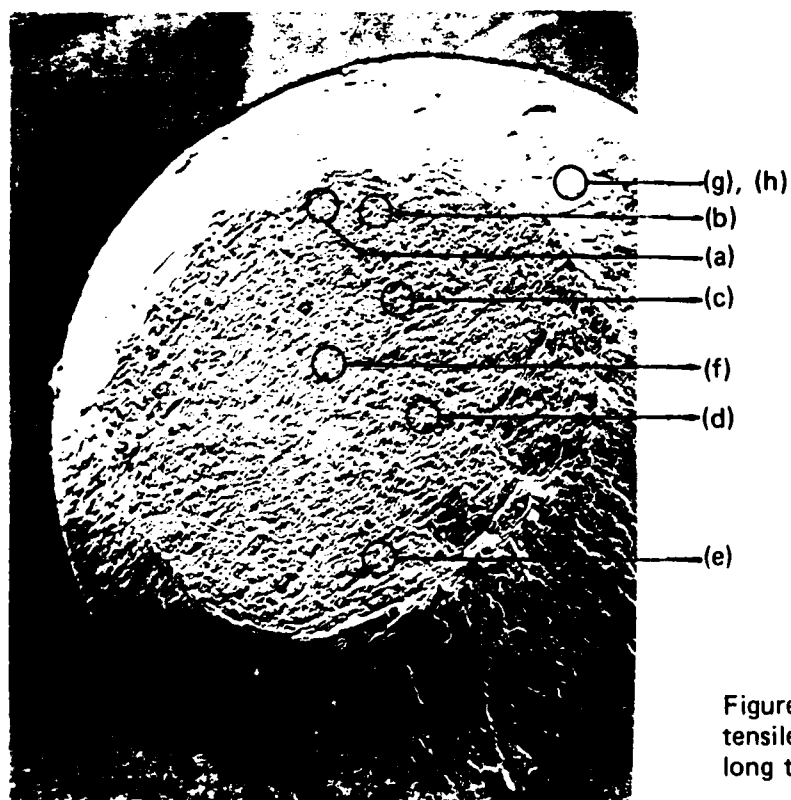


Figure 3. SEM long transverse tensile fractographs. ESR 300M, long transverse.



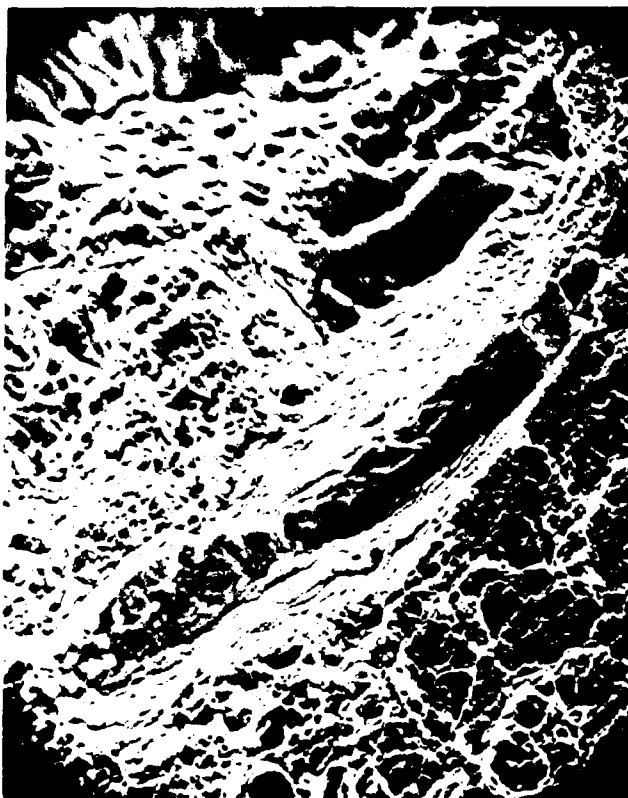
(a)

1000X

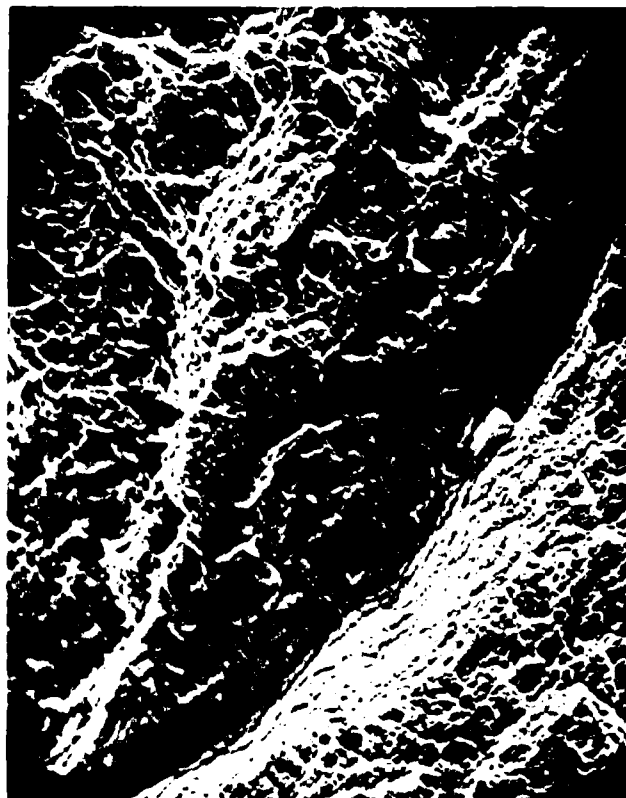


(b)

200X



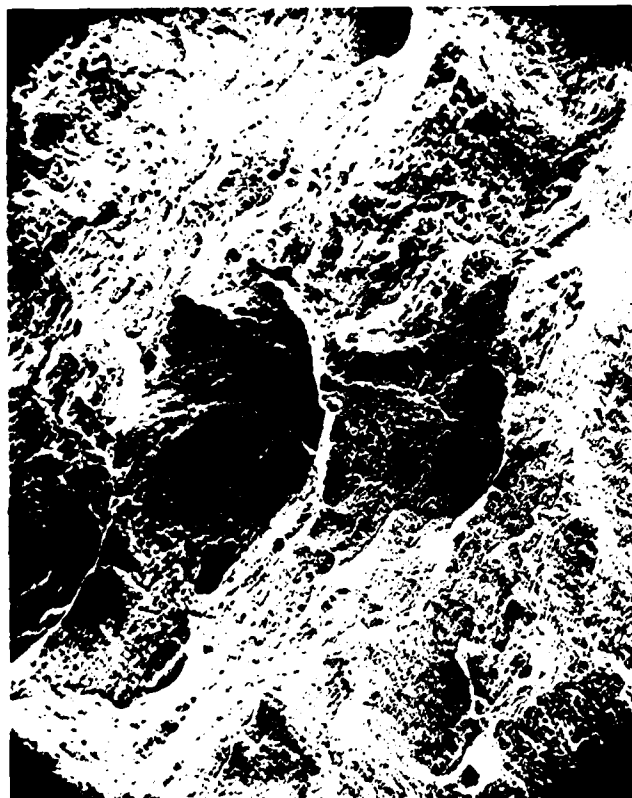
2000X



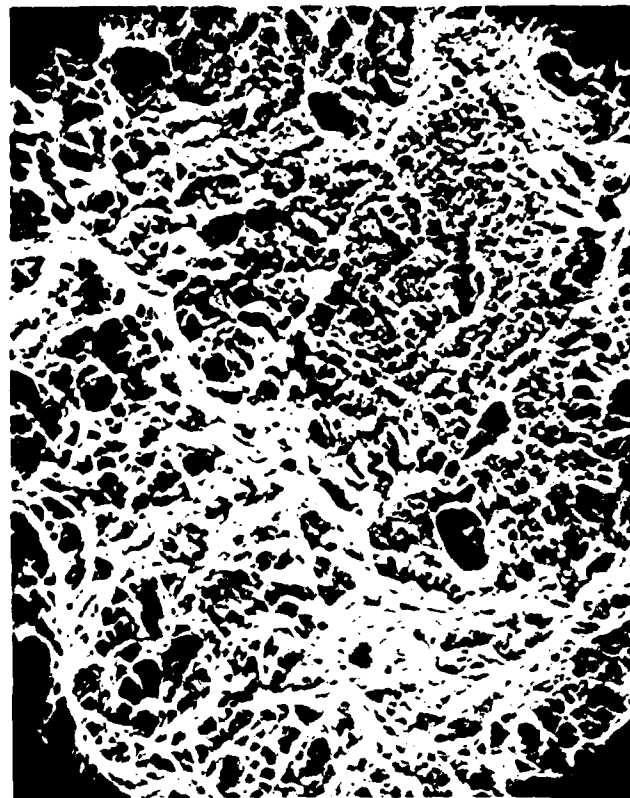
(d)

2000X

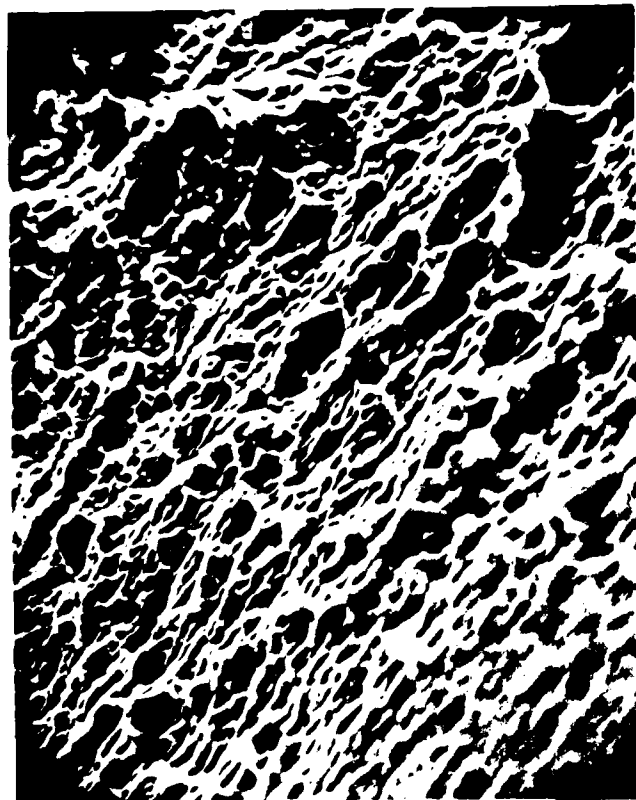
Figure 3. ESR 300M, long transverse (cont.).



(e) 200X



(f) 2000X

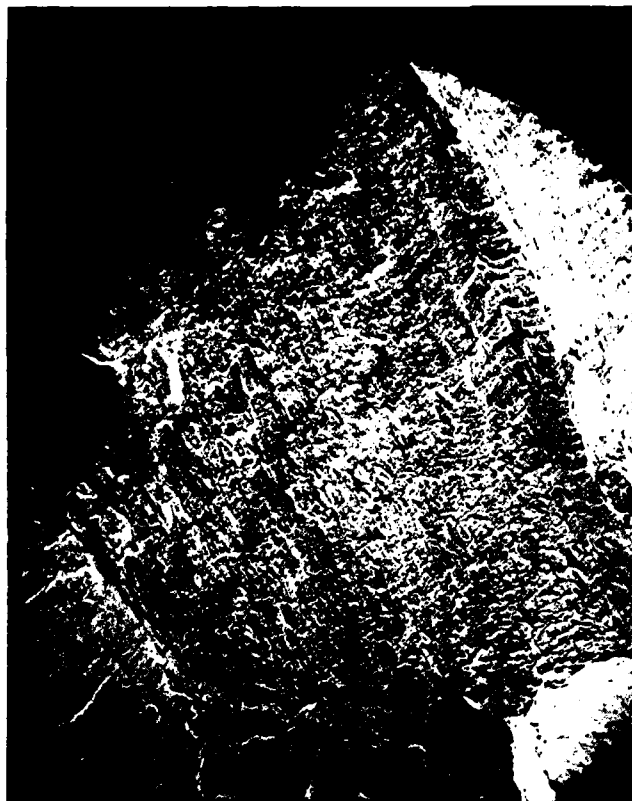


(g) 5000X



(h) 500X

Figure 3. ESR 300M, long transverse (cont.).



20X

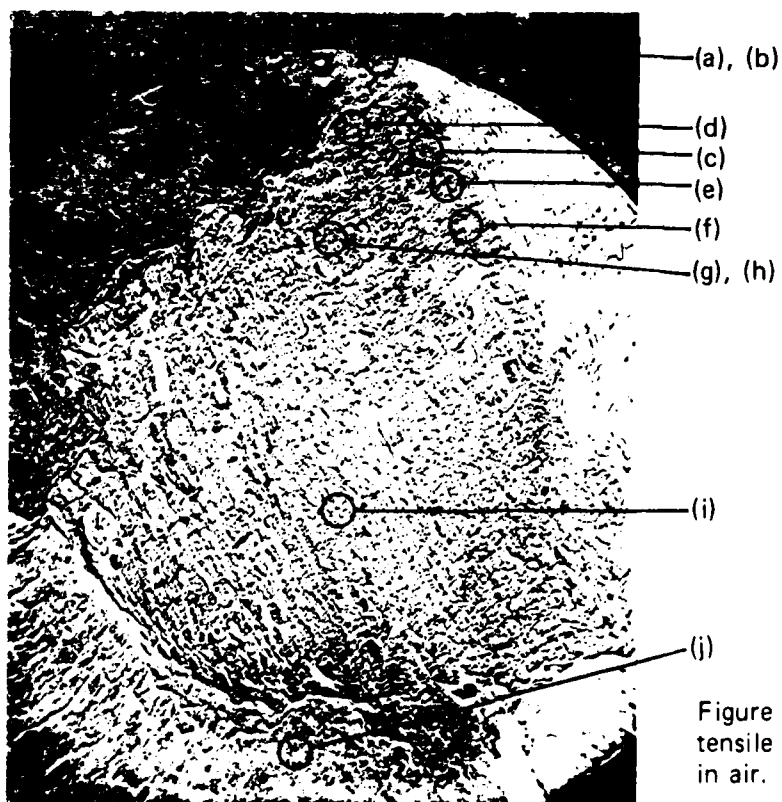
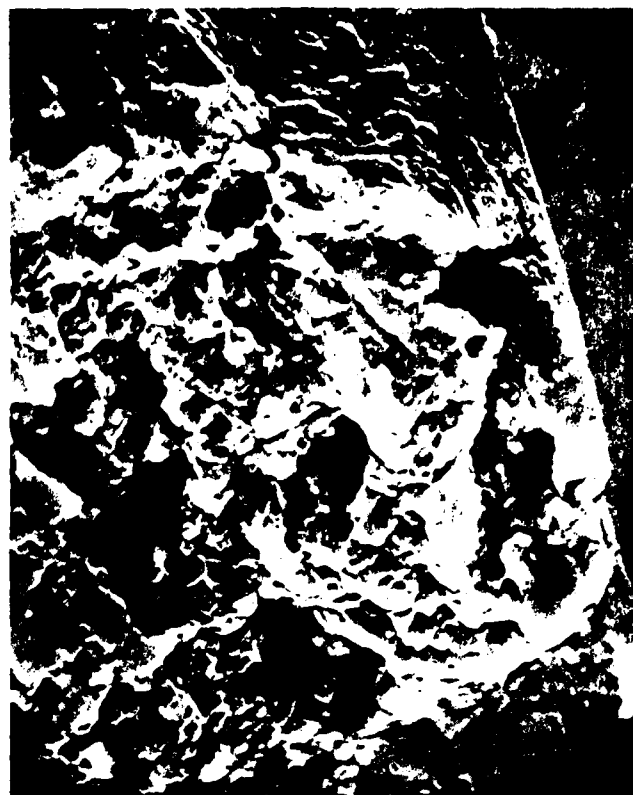


Figure 4. SEM short transverse tensile fractographs - heat treated in air. Short transverse.



(a) 1000X



(b) 5000X



(c) 1000X



(d) 5000X

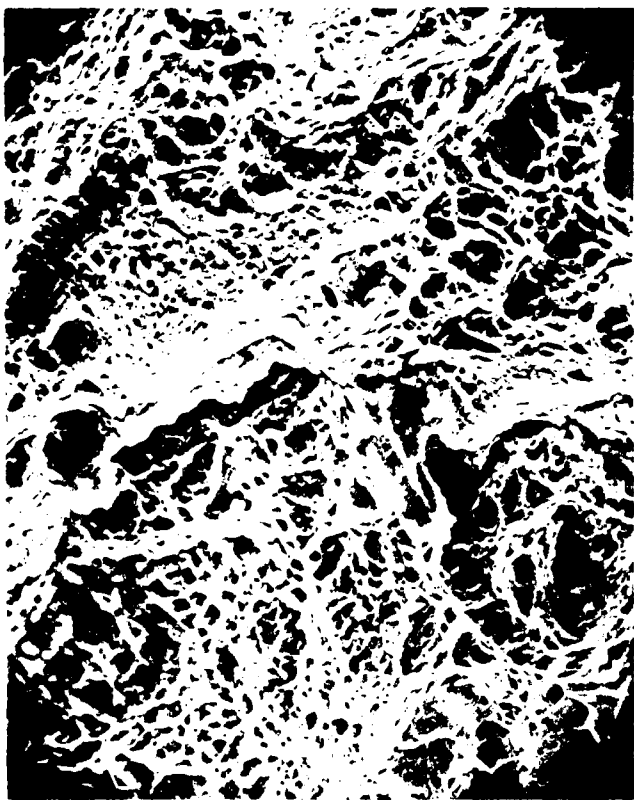
Figure 4. ESR 300M, short transverse (cont.).



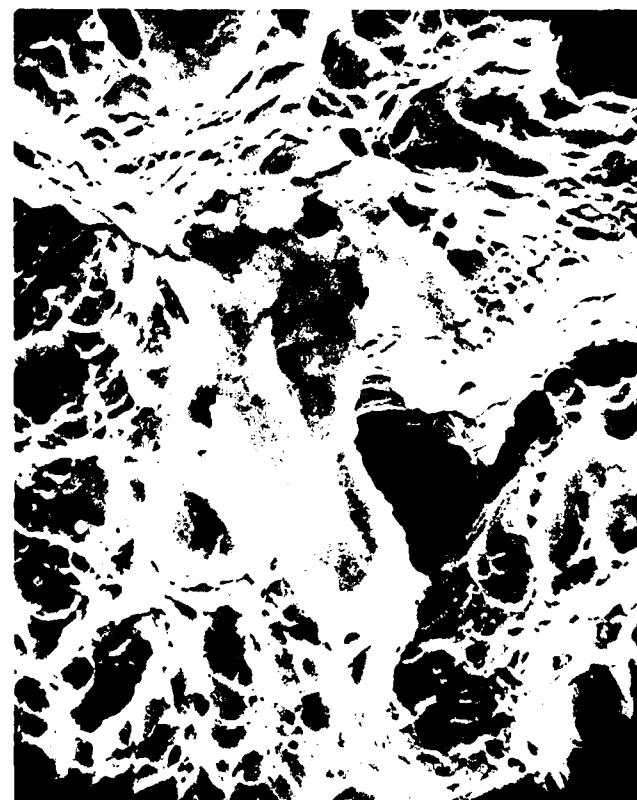
(e) 200X



(f) 500X

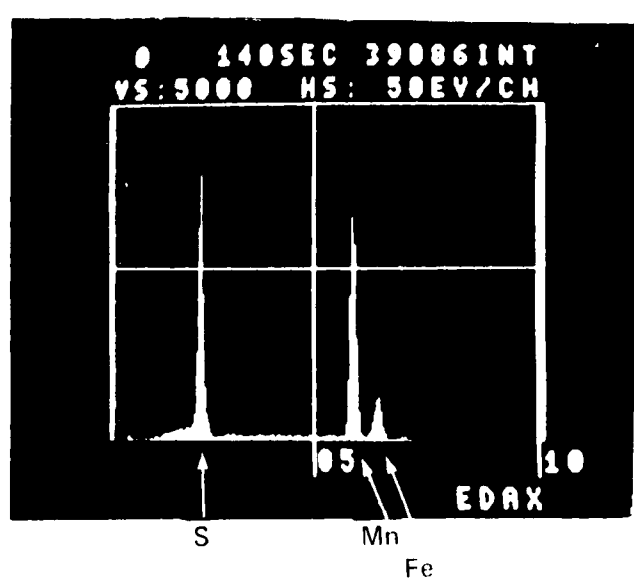
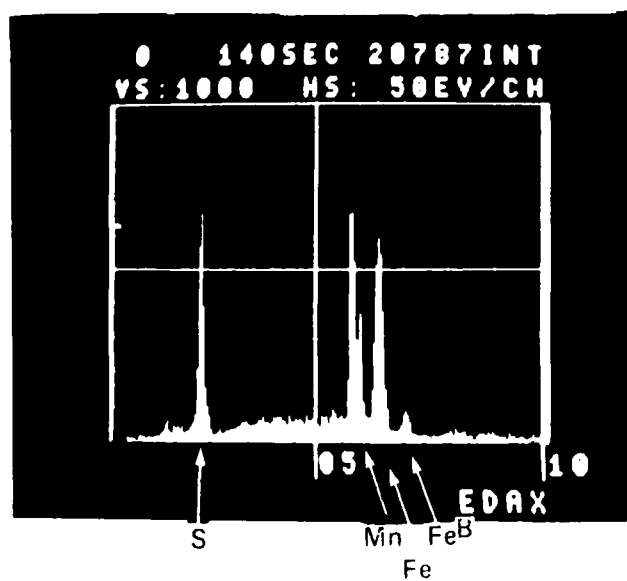
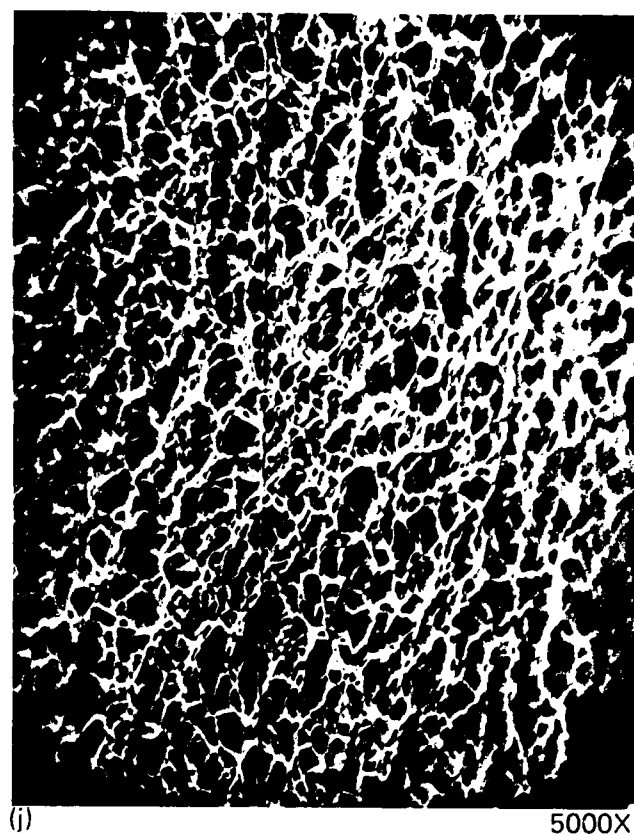
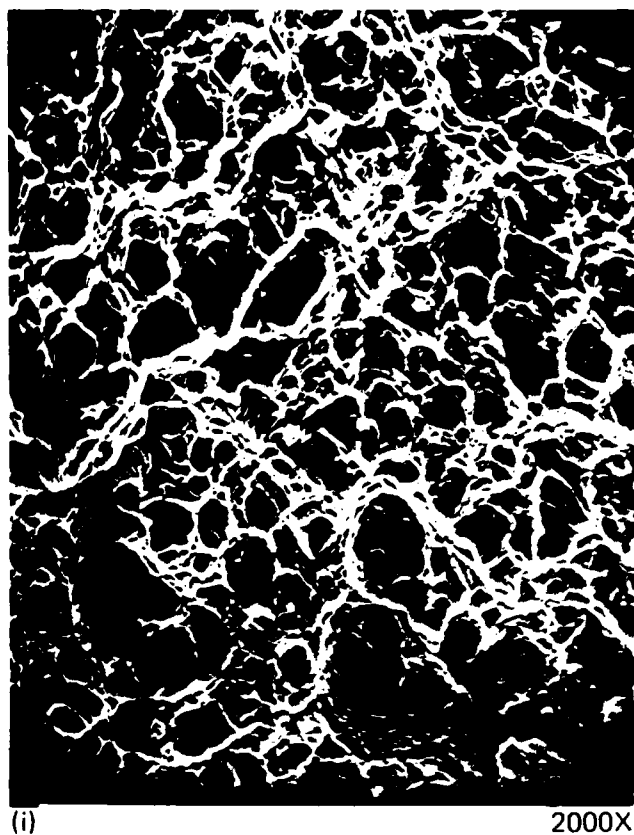


2000X



5000X

Figure 4. ESR 300M, short transverse (cont.).



(k) SEM spectrometer trace of inclusion shown in Figure 4(c).

Figure 4. ESR 300M, short transverse (cont.).



20X



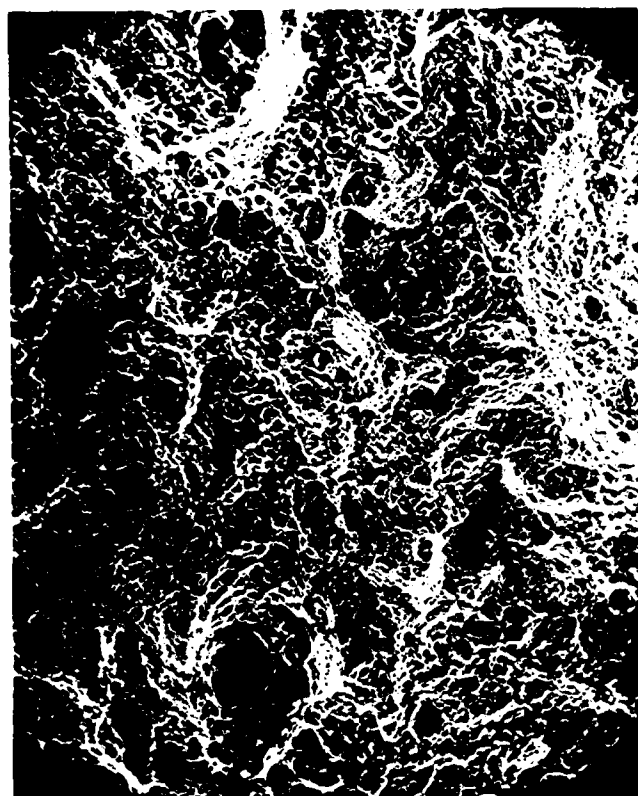
(e), (f)

(a), (b)

(c), (d)

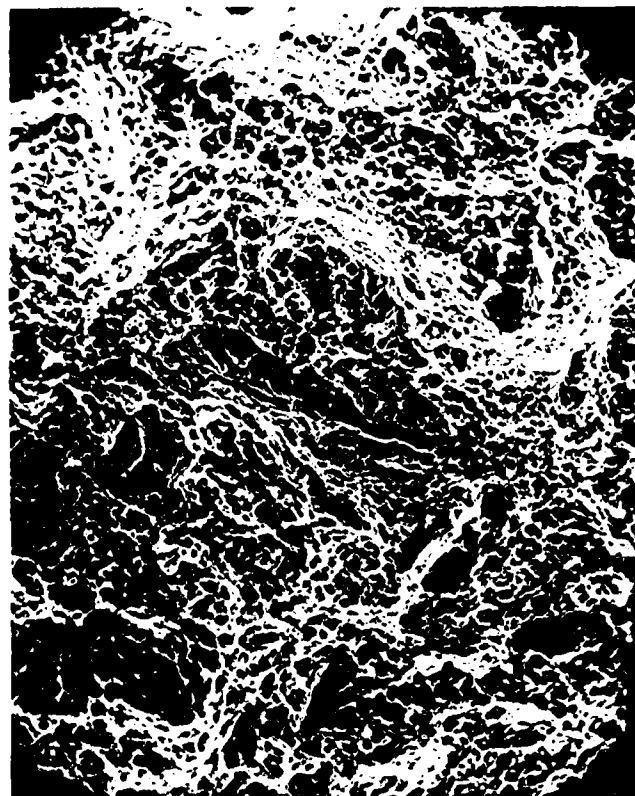
(g), (h)

Figure 5. SEM short transverse tensile fractographs - heat treated in air. ESR 300M, short transverse.



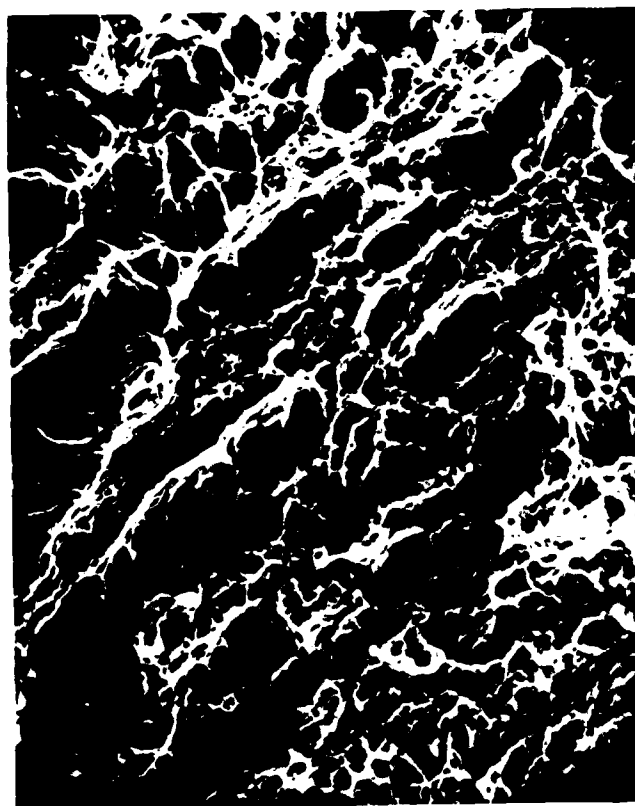
(a)

500X



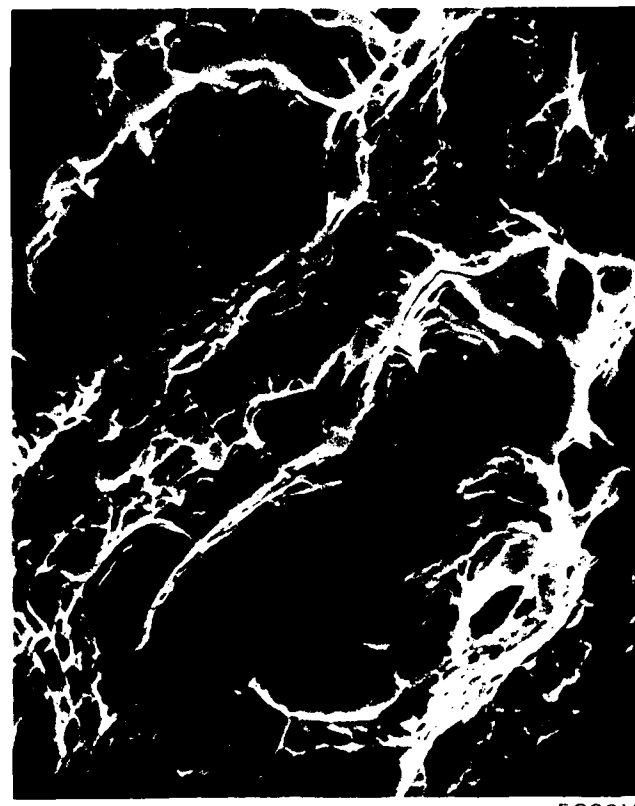
(b)

1000X



(c)

2000X



(d)

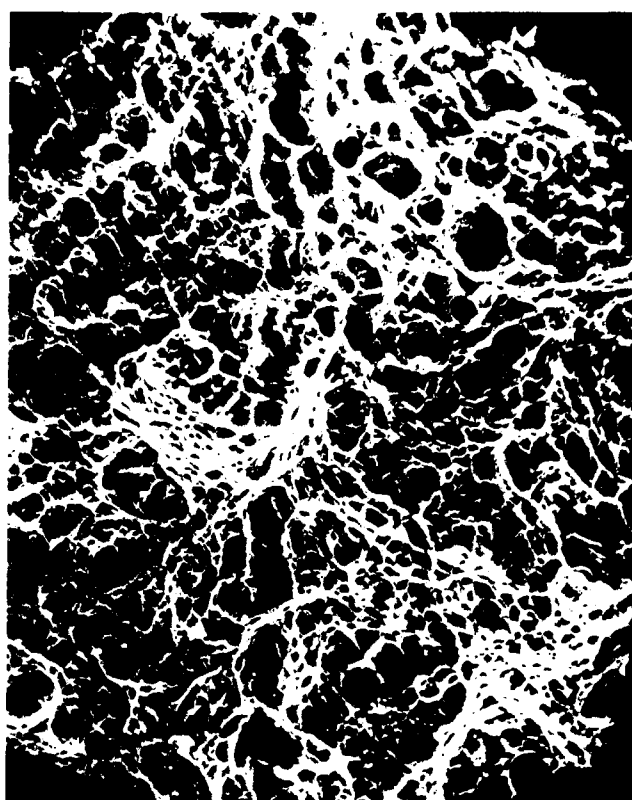
5000X

Figure 5. ESR 300M, short transverse (cont.).



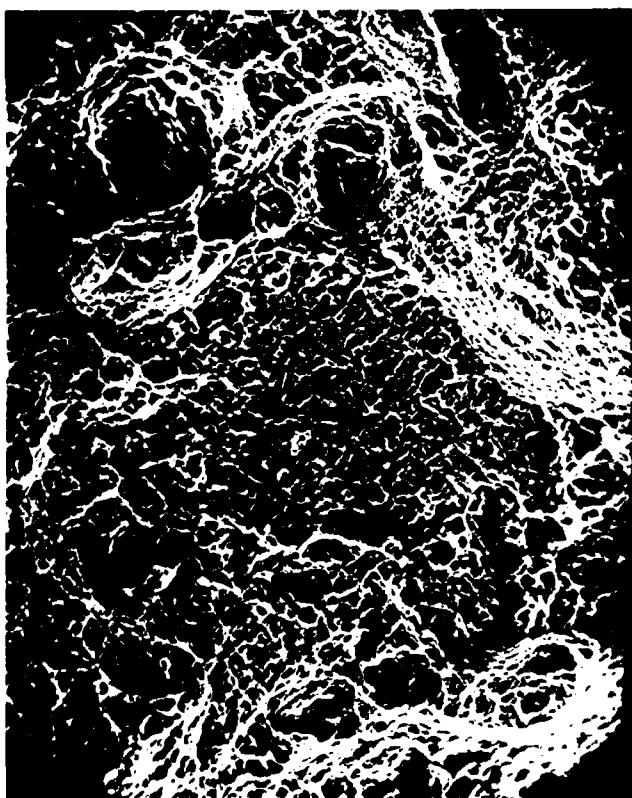
(e)

2000X



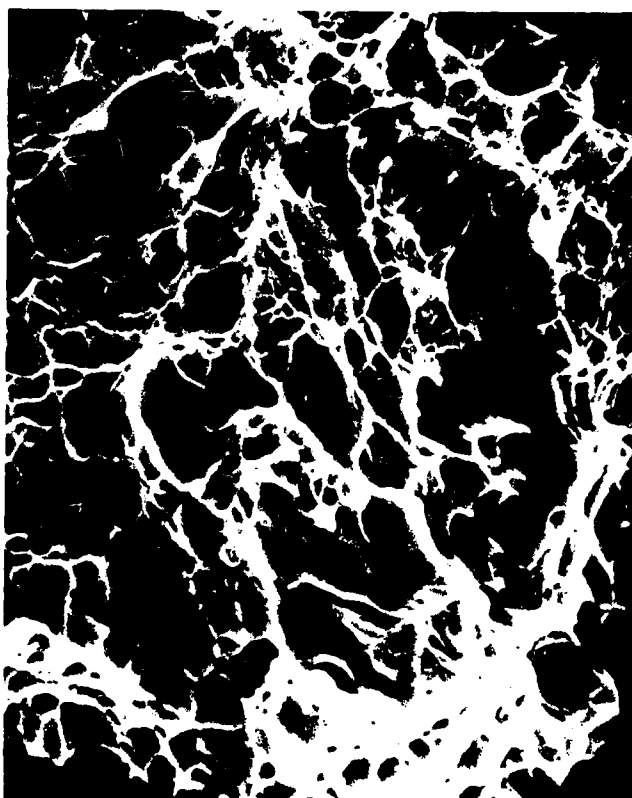
(f)

2000X



(g)

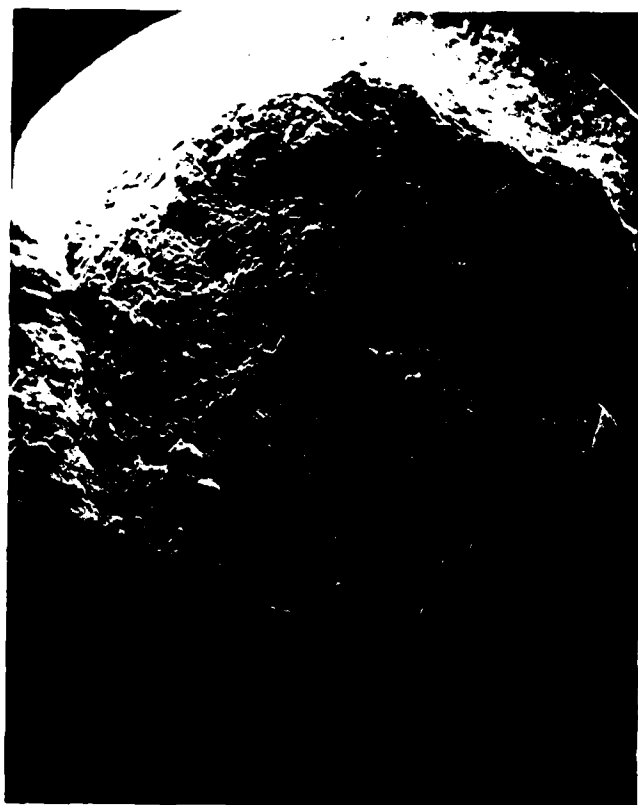
1000X



(h)

5000X

Figure 5. ESR 300M, short transverse (cont.).



20X

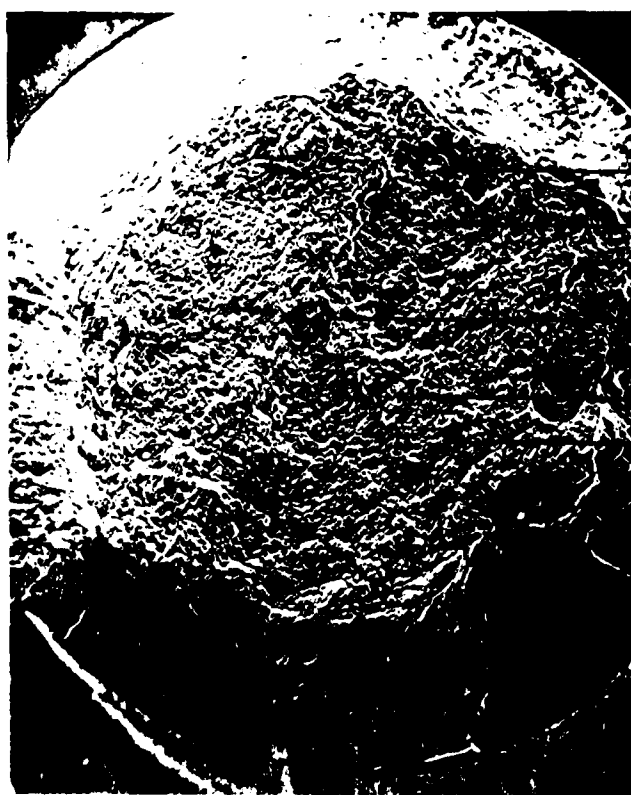
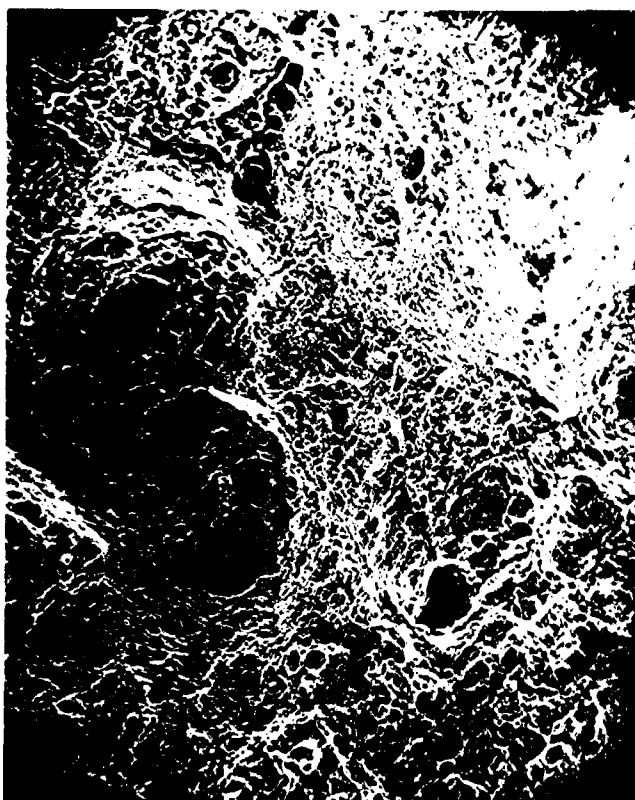
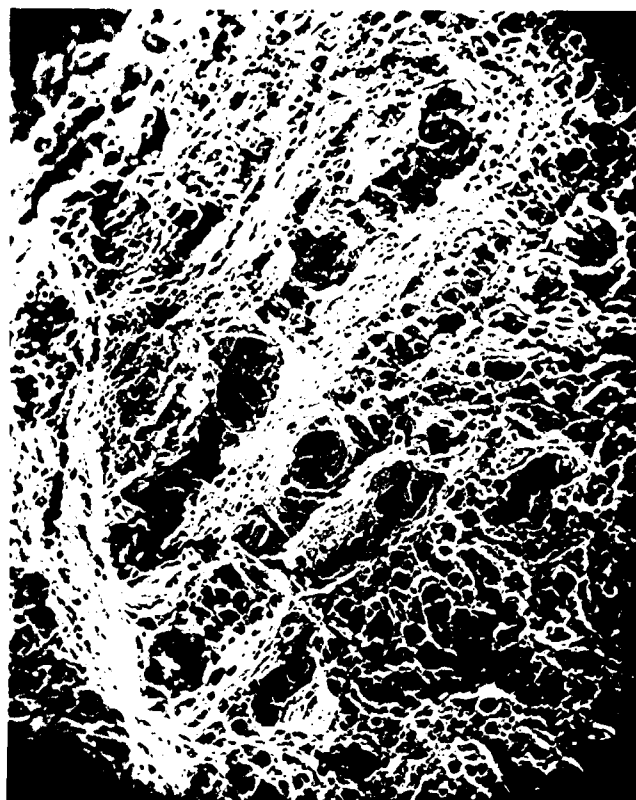


Figure 6. SEM short transverse tensile fractographs - heat treated in vacuum. ESR 300M, short transverse - Vac. H.T.



(a)

500X



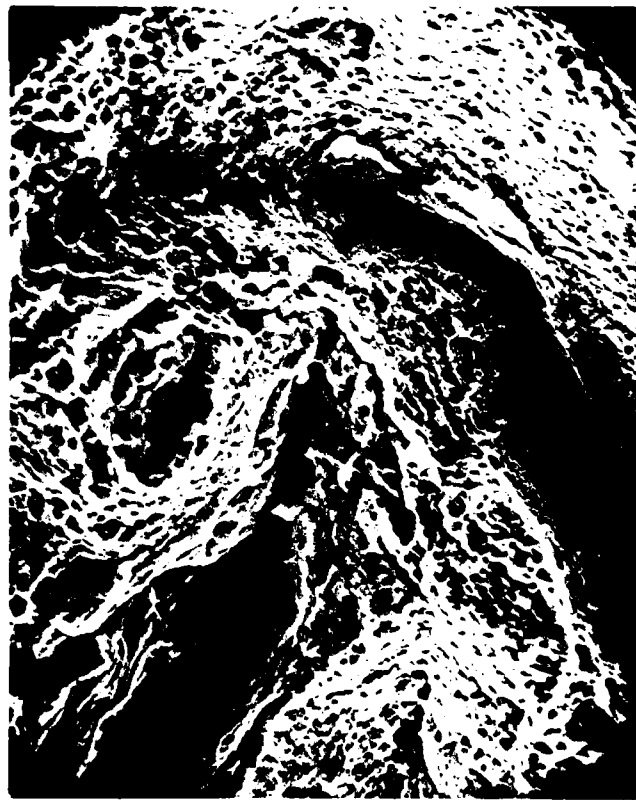
(b)

1000X



(c)

1000X



(d)

2000X

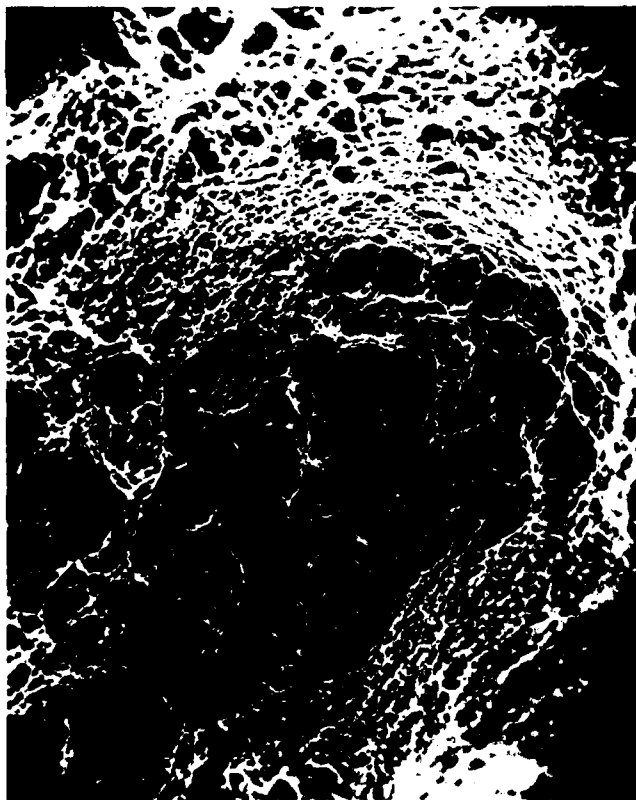
Figure 6. ESR 300M, short transverse Vac. H.T. (cont.).



(e) 1000X



(f) 2000X

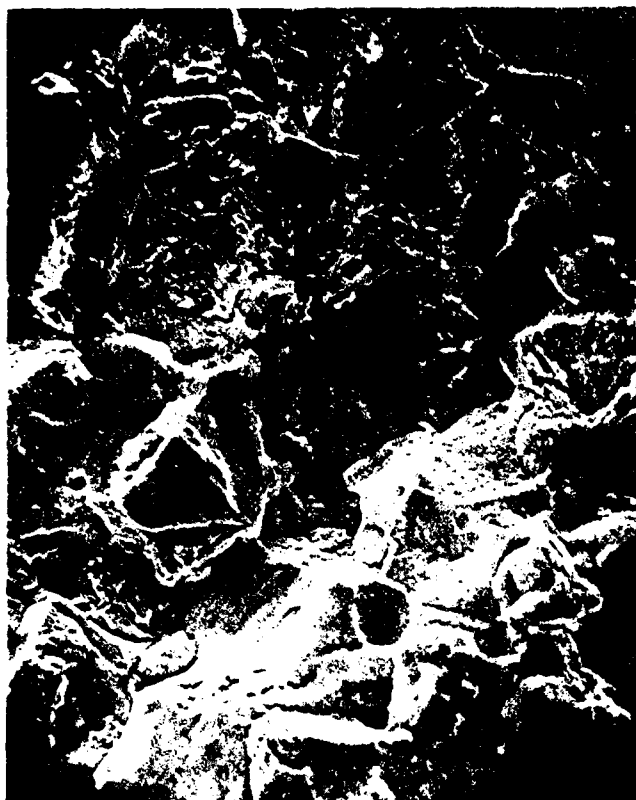


(g) 1000X

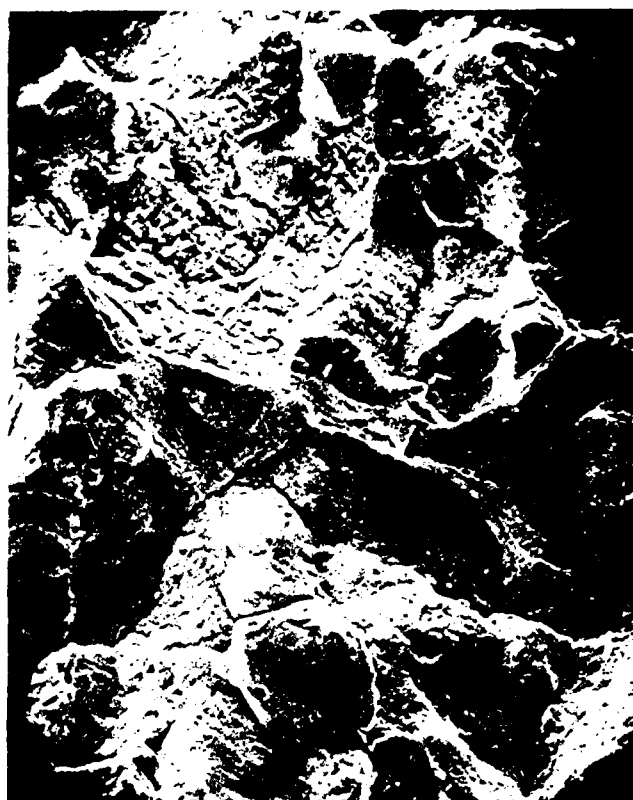


(h) 2000X

Figure 6. ESR 300M, short transverse - Vac. H.T. (cont.).



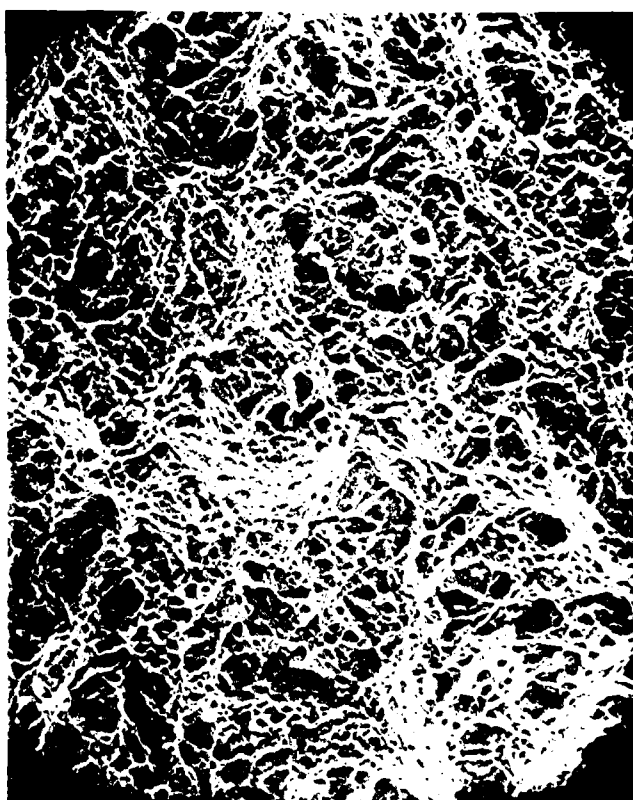
(a) 1000X



(b) 1000X



(c) 1000X



(d) 1000X

Figure 7. Stress corrosion cracking, ESR 300M.

DISTRIBUTION LIST

No. of Copies	To
1	Office of the Under Secretary of Defense for Research and Engineering, The Pentagon, Washington, DC 20301
12	Commander, Defense Technical Information Center, Cameron Station, Building 5, 5010 Duke Street, Alexandria, VA 22314
	Metals and Ceramics Information Center, Battelle Columbus Laboratories, 505 King Avenue, Columbus, OH 43201
1	ATTN: J. H. Brown, Jr.
	Deputy Chief of Staff, Research, Development, and Acquisition, Headquarters, Department of the Army, Washington, DC 20301
1	ATTN: DAMA-ARZ
	Commander, Army Research Office, P.O. Box 12211, Research Triangle Park, NC 27709
1	ATTN: Information Processing Office
	Commander, U.S. Army Materiel Development and Readiness Command, 5001 Eisenhower Avenue, Alexandria, VA 22333
1	ATTN: DRCLDC
	Commander, U.S. Army Materiel Systems Analysis Activity, Aberdeen Proving Ground, MD 21005
1	ATTN: DRXSY-MP, Director
	Commander, U.S. Army Missile Command, Redstone Arsenal, AL 35809
1	ATTN: Technical Library
1	DRSMI-CS, R. B. Clem
	Commander, U.S. Army Armament Research and Development Command, Dover, NJ 07801
2	ATTN: Technical Library
1	DRDAR-SCM, J. D. Corrie
1	Dr. J. Waldman
	Commander, U.S. Army Tank-Automotive Command, Warren, MI 48090
1	ATTN: DRSTA-RKA
2	DRSTA-UL, Technical Library
1	DRSTA-RCK
	Commander, U.S. Army Foreign Science and Technology Center, 220 7th Street, N.E., Charlottesville, VA 22901
1	ATTN: Military Tech, Mr. Marley
	Director, Eustis Directorate, U.S. Army Air Mobility Research and Development Laboratory, Fort Eustis, VA 23604
1	ATTN: DAVDL-E-MOS
1	DAVDL-EU-TAP

No. of
Copies

To

U.S. Army Aviation Training Library, Fort Rucker, AL 36360
1 ATTN: Building 5906--5907

Commander, U.S. Army Aviation Research and Development Command,
4300 Goodfellow Boulevard, St. Louis, MO 63120
1 ATTN: DRDAV-EGX
1 DRDAV-EX, Mr. R. Lewis
1 DRDAV-EQ, Mr. Crawford
1 DRCPM-AAH-TM, Mr. R. Hubbard
1 DRDAV-DS, Mr. W. McClane

Naval Research Laboratory, Washington, DC 20375
1 ATTN: Dr. J. M. Krafft - Code 5830
1 Code 2627

Chief of Naval Research, Arlington, VA 22217
1 ATTN: Code 471

Commander, U.S. Air Force Wright Aeronautical Laboratories,
Wright-Patterson Air Force Base, OH 45433
2 ATTN: AFWAL/MLSE, E. Morrissey
1 AFWAL/MLC
1 AFWAL/MLLP
1 AFWAL/MLBC
1 AFWAL/MLXE

Aeronautical Systems Division (AFSC), Wright-Patterson Air Force Base,
OH 45433
1 ATTN: ASD/ENFEF, D. C. Wight
1 ASD/ENFTV, D. J. Wallick
1 ASD/XRHD, G. B. Bennett

Air Force Armament Laboratory, Eglin Air Force Base, FL 32542
1 ATTN: AFATL/DLYA, V. D. Thornton

Air Force Flight Dynamics Laboratory, Wright-Patterson Air Force Base,
OH 45433
1 ATTN: AFFDL/FES, G. W. Ducker
1 AFFDL/FES, J. Hodges
1 AFFDL/TST, Library

Air Force Test and Evaluation Center, Kirtland Air Force Base, NM 87115
1 ATTN: AFTEC-JT

NASA - Ames Research Center, Army Air Mobility Research and Development
Laboratory, Mail Stop 207-5, Moffett Field, CA 94035
1 ATTN: SAVDL-AS-X, F. H. Immen

No. of Copies	To
1	Naval Air System Command, Department of the Navy, Washington, DC 20360
1	ATTN: AIR-03PAF
1	AIR-5203
1	AIR-5204J
1	AIR-530313
1	Naval Material Command, Washington, DC 20360
1	ATTN: MAT-0331
1	Naval Post Graduate School Monterey, CA 93948
1	ATTN: Code 57BP, R. E. Ball
1	Naval Surface Weapons Center, Dahlgren Laboratory, Dahlgren, VA 22448
1	ATTN: Code G-54, Mr. J. Hall
1	Code G-54, Mr. E. Rowe
1	Naval Weapons Center, China Lake, CA 93555
1	ATTN: Code 40701
1	Code 3624
1	Commander, Rock Island Arsenal, Rock Island, IL 61299
1	ATTN: DRSAR-PPV
1	Beech Aircraft Corporation, 9709 E. Central Avenue, Wichita, KS 67206
1	ATTN: Engineering Library
1	Bell Helicopter Company, A Textron Company, P.O. Box 482, Fort Worth, TX 76101
1	ATTN: J. R. Johnson
1	Boeing Vertol Company, A Division of the Boeing Company, P.O. Box 16858, Philadelphia, PA 19142
1	ATTN: J. E. Gonsalves, M/S P32-19
1	Calspan Corporation, P.O. Box 235, Buffalo, NY 14221
1	ATTN: Library
1	Cessna Aircraft Company, Wallace Division, P.O. Box 1977, Wichita, KS 67201
1	ATTN: B. B. Overfield
1	Fairchild Industries, Inc., Fairchild Republic Company, Conklin Street, Farmingdale, Long Island, NY 11735
1	ATTN: Engineering Library, G. A. Mauter
1	Falcon Research and Development Company, 601 San Pedro, N.E., Suite 205, Albuquerque, NM 87108
1	ATTN: W. L. Baker
1	General Dynamics Corporation, Convair Division, P.O. Box 80877, San Diego, CA 92138
1	ATTN: Research Library, U. J. Sweeney

No. of
Copies

To

General Research Corporation, Science and Technology Division,
5383 Hollister Avenue, P.O. Box 3587, Santa Barbara, CA 93105
1 ATTN: R. Rodman

Gruman Aerospace Corporation, South Oyster Bay Road, Bethpage, NY 11714
1 ATTN: Technical Information Center, J. Davis

Hughes Helicopters, A Division of Summa Corporation, Centinela & Teale Street,
Culver City, CA 90230
1 ATTN: Library, 2/T2124, D. K. Goss
1 Mr. A. Hirko
1 Mr. L. Soffa
1 Mr. A. Edwards

IIT Research Institute, 10 West 35th Street, Chicago, IL 60616
1 ATTN: K. McKee

Kaman Aerospace Corporation, Old Winsor Road, Bloomfield, CT 06002
1 ATTN: H. E. Showalter

Lockheed-California Company, A Division of Lockheed Aircraft Corporation,
Burbank, CA 91503
1 ATTN: Technological Information Center, 84-40, U-35, A-1

Vought Corporation, P.O. Box 5907, Dallas, TX 75232
1 ATTN: D. M. Reedy, 2-30110
1 M. P. Poulos, Jr.

McDonnell Douglas Corporation, 3855 Lakewood Boulevard, Long Beach, CA 90846
1 ATTN: Technical Library, C1 290/36-84

Northrop Corporation, Aircraft Division, 3901 W. Broadway, Hawthorne, CA 90250
1 ATTN: Mgr. Library Services, H. W. Jones

Parker Hannifin Corporation, Bertea Control Systems Division,
18001 Von Karman Avenue, Irvine, CA 92715
1 ATTN: C. Beneker

Rockwell International Corporation, Los Angeles Aircraft Division,
B-1 Division, International Airport, Los Angeles, CA 90009
1 ATTN: W. L. Jackson

Sikorsky Aircraft, A Division of United Aircraft Corporation, Main Street,
Stratford, CT 06602
1 ATTN: J. B. Faulk
1 W. G. Degnan

Teledyne CAE, 1330 Laskey Road, Toledo, OH 43697
1 ATTN: Librarian, M. Dowdell

Simonds Steel Division, Guterl Special Steel Corporation, Lockport, NY 14094
1 ATTN: Mr. R. Farrington

No. of
Copies

To

Georgia Institute of Technology, School of Mechanical Engineering,
Atlanta, GA 30332
1 ATTN: Dr. J. T. Berry

Lukens Steel Company, Coatesville, PA 19320
1 ATTN: Dr. R. S. Swift

Republic Steel Corporation, 410 Oberlin Avenue SW, Massillon, OH 44646
1 ATTN: Mr. R. Sweeney
1 Mr. W. H. Brechtel
1 Mr B. G. Hughes

METTEC, 1805 E. Carnegie Avenue, Santa Ana, CA 92705
1 ATTN: Dr. L. Raymond

Ingersoll Rand Oilfield Products Division, P.O. Box 1101, Pampa, TX 79065
1 ATTN: Mr. W. L. Hallerberg

Director, Army Materials and Mechanics Research Center, Watertown, MA 02172
2 ATTN: DRXMR-PL
1 Author

Army Materials and Mechanics Research Center,
WATERLOO, MASSACHUSETTS 02127
MECHANICAL PROPERTIES AND FRACTOGRAPHY
OF ELECTROSLAG REMELTED 300M STEEL -
Albert R. Anderson

Technical Report AMMR-TR 53-13, March 1963, 28 pp -
Contracting Office Project 1162154P04
AMMR Code 61106, 604711

Steel, 300M
Mechanical properties
Fractography

Engineering and stress corrosion cracking properties, with microscopic examination of fracture surfaces, are presented for a high strength electroslag remelted 300M steel. Comparisons are made of electroslag remelted 4340 steel and electroslag and vacuum arc remelted 300M and 4340 steels. Electroslag remelted 300M steel at high vacuum levels can achieve the mechanical property levels obtained by vacuum arc remelting in the longitudinal orientation. However, the short transverse ductility of electroslag remelted 300M steel varies considerably and can be unacceptably low. Scanning electron microscopic examination of short transverse tensile specimens having good ductility did not reveal any fractographic differences that could be related to the heat treatment process. Impact energy varied with orientation. An improvement in stress corrosion cracking susceptibility was obtained over VAR 4340 steel.

Army Materials and Mechanics Research Center,
WATERLOO, MASSACHUSETTS 02127
MECHANICAL PROPERTIES AND FRACTOGRAPHY
OF ELECTROSLAG REMELTED 300M STEEL -
Albert R. Anderson

Technical Report AMMR-TR 53-13, March 1963, 28 pp -
Contracting Office Project 1162154P04
AMMR Code 61106, 604711

Steel, 300M
Mechanical properties
Fractography

Engineering and stress corrosion cracking properties, with microscopic examination of fracture surfaces, are presented for a high strength electroslag remelted 300M steel. Comparisons are made of electroslag remelted 4340 steel and electroslag and vacuum arc remelted 300M and 4340 steels. Electroslag remelted 300M steel at high vacuum levels can achieve the mechanical property levels obtained by vacuum arc remelting in the longitudinal orientation. However, the short transverse ductility of electroslag remelted 300M steel varies considerably and can be unacceptably low. Scanning electron microscopic examination of short transverse tensile specimens having good ductility did not reveal any fractographic differences that could be related to the heat treatment process. Impact energy varied with orientation. An improvement in stress corrosion cracking susceptibility was obtained over VAR 4340 steel.

Army Materials and Mechanics Research Center,
WATERLOO, MASSACHUSETTS 02127
MECHANICAL PROPERTIES AND FRACTOGRAPHY
OF ELECTROSLAG REMELTED 300M STEEL -
Albert R. Anderson

Technical Report AMMR-TR 53-13, March 1963, 28 pp -
Contracting Office Project 1162154P04
AMMR Code 61106, 604711

Engineering and stress corrosion cracking properties, with microscopic examination of fracture surfaces, are presented for a high strength electroslag remelted 300M steel. Comparisons are made of electroslag remelted 4340 steel and electroslag and vacuum arc remelted 300M and 4340 steels. Electroslag remelted 300M steel at high vacuum levels can achieve the mechanical property levels obtained by vacuum arc remelting in the longitudinal orientation. However, the short transverse ductility of electroslag remelted 300M steel varies considerably and can be unacceptably low. Scanning electron microscopic examination of short transverse tensile specimens having good ductility did not reveal any fractographic differences that could be related to the heat treatment process. Impact energy varied with orientation. An improvement in stress corrosion cracking susceptibility was obtained over VAR 4340 steel.

Army Materials and Mechanics Research Center,
WATERLOO, MASSACHUSETTS 02127
MECHANICAL PROPERTIES AND FRACTOGRAPHY
OF ELECTROSLAG REMELTED 300M STEEL -
Albert R. Anderson

Technical Report AMMR-TR 53-13, March 1963, 28 pp -
Contracting Office Project 1162154P04
AMMR Code 61106, 604711

Engineering and stress corrosion cracking properties, with microscopic examination of fracture surfaces, are presented for a high strength electroslag remelted 300M steel. Comparisons are made of electroslag remelted 4340 steel and electroslag and vacuum arc remelted 300M and 4340 steels. Electroslag remelted 300M steel at high vacuum levels can achieve the mechanical property levels obtained by vacuum arc remelting in the longitudinal orientation. However, the short transverse ductility of electroslag remelted 300M steel varies considerably and can be unacceptably low. Scanning electron microscopic examination of short transverse tensile specimens having good ductility did not reveal any fractographic differences that could be related to the heat treatment process. Impact energy varied with orientation. An improvement in stress corrosion cracking susceptibility was obtained over VAR 4340 steel.

END

FILMED

7-83

DTIC